

## LOCAL STRUCTURE OF ICOSAHEDRAL AND AMORPHOUS Al-Mn ALLOYS

J.B. BOYCE, F.G. BRIDGES\* and J.J. HAUSER\*\*

*Xerox Palo Alto Research Center, Palo Alto, CA 94304, U.S.A.**\*Department of Physics, University of California, Santa Cruz, CA 95064, U.S.A.**\*\*AT&T Bell Laboratories, Murray Hill, NJ 07974, U.S.A.*

**Résumé.** – Nous comparons les mesures EXAFS au seuil d'absorption K du manganèse entre Al-Mn icosahédrique (i), amorphe (a) et cristallin (c). Les phases i et a présentent des distributions de proches voisins Mn-Al, très similaires. Ces distributions sont trouvées plus larges et plus asymétriques que dans la phase c. L'asymétrie de la phase a est quelque peu moins prononcée que celle associée à la phase i. Toutes les phases ont environ 10 atomes Al premiers voisins des atomes Mn.

**Abstract.** – EXAFS measurements on the Mn K edge of icosahedral (i), amorphous (a), and crystalline (c) Al-Mn are compared. It is found that the i- and a-phases have very similar Mn-Al near neighbor distributions, both of which are broader and more asymmetric than that for the c-phase. The asymmetry for the a-phase is somewhat less pronounced than that for the i-phase. All phases have approximately 10 Al first neighbors to the Mn atoms.

The discovery of five-fold rotational symmetry in rapidly quenched metal alloys of Al-Mn [1] and other materials [2] has generated considerable interest. The sharpness of the diffraction spots indicates that the alloys possess long-range orientational order belonging to the icosahedral point group, one that is inconsistent with long-range translational symmetry. A number of models have been proposed to explain these results, ranging from perfect quasiperiodic tiling [3] in three dimensions to twinning [4]. Yet a detailed model for the location of the constituent atoms has not been determined. Nonetheless, information on the microscopic atomic arrangement has been derived using several local probes, namely, Mossbauer [5], NMR [6], and EXAFS [7-10]. This information goes a long way toward a detailed understanding of the local atomic arrangement.

To further elucidate the nature of the local structure, we have performed EXAFS measurements on  $Al_{1-x}Mn_x$  quasicrystals, with x from 12 atomic % to 20 atomic %, and have compared these results with those on amorphous  $Al_{0.85}Mn_{0.15}$ , on crystalline  $Al_6Mn$  and on dilute alloys of Mn in Al. Also, since it has been observed that small amounts of Si appear to enhance the stability of the icosahedral phase of Al-Mn, we have measured the EXAFS on icosahedral  $Al_{0.74}Mn_{0.20}Si_{0.06}$  for comparison.

The icosahedral samples were prepared by rapid quenching on a rotating metal wheel. The samples contained 12 atomic %, 15%, 16%, and 20% Mn, and were approximately 2 mm wide by 30  $\mu$ m thick. The 12% and 15% materials were checked by electron diffraction to verify the icosahedral phase and by energy dispersive diffraction to verify that they were free of other phases. Part of the  $Al_{0.85}Mn_{0.15}$  quasicrystalline material was annealed at 640°C for one hour to form crystalline  $Al_6Mn$ . Also dilute alloys of Al containing 0.4 atomic %, 3%, 4%, 5%, and 6% Mn were prepared by rapid quenching. The 6 at. % sample contained some icosahedral phase but the lower concentration dilute alloys consisted of only FCC Al containing Mn. The amorphous sample, a- $Al_{0.85}Mn_{0.15}$ , was prepared by sputtering from the corresponding induction-melt alloy onto a NaCl substrate. The NaCl was dissolved away, leaving a film of about 30  $\mu$ m thickness.

The EXAFS measurements were performed on the Mn K edge at both 4.2K and 77K using a Si(111) double crystal monochromator on a wiggler beam line at SSRL. The transmission data was reduced in the standard way [11], being converted to k-space and Fourier-transformed to real space.

The EXAFS results on the various samples were compared. The Fourier transform of the EXAFS,  $X(k)$ , multiplied by  $k^3$ , is shown in Fig. 1 for, from top to bottom,  $\text{Al}_6\text{Mn}$ ,  $a\text{-Al}_{0.85}\text{Mn}_{0.15}$ ,  $i\text{-Al}_{0.86}\text{Mn}_{0.14}$ , and  $i\text{-Al}_{0.74}\text{Mn}_{0.20}\text{Si}_{0.06}$ . It is seen that the data on the latter two samples,  $i\text{-AlMn}$  and  $i\text{-AlMnSi}$ , are very similar, not only for the first neighbor peak, but also for the second and third neighbors. This is also true, with only small differences, for the other icosahedral alloys with differing Mn content. A difference occurs in the first neighbor peak which has an oscillatory feature in the amplitude for the Si-stabilized sample but not for  $i\text{-AlMn}$ . This oscillation may be due to noise or due to the presence of the Si in the first neighbor environment. In any event, it is a comparatively small feature, indicating that the local environment is quite similar in the two icosahedral materials.

The amorphous phase differs from the  $i$ -phase in two respects. First, the first neighbor peak for  $a\text{-AlMn}$  is larger and sharper, indicating a narrower Mn-Al first-neighbor environment. The phases of the EXAFS of the two peaks are similar, implying that the shape of the distributions is the same. Second, the further neighbor peaks are greatly reduced in  $a\text{-AlMn}$ , consistent with a more distorted further neighbor distribution, as is to be expected.

The data on all three of these samples differ substantially from that of crystalline  $\text{Al}_6\text{Mn}$ . The first neighbor peaks differ in amplitude and phase, indicating a different shape of the distribution. These differences and similarities are also evident in the Fourier-filtered first-neighbor  $k$ -space data [8]. A major point to make is that the phase of the EXAFS of the crystalline and icosahedral materials differ beyond about  $k = 8 \text{ \AA}^{-1}$ , suggesting a more asymmetric first neighbor pair distribution function,  $p(r)$ , for the latter [8]. Also the phases of  $X(k)$  for the amorphous and icosahedral materials are the same, implying a similar asymmetry in their  $p(r)$ 's.

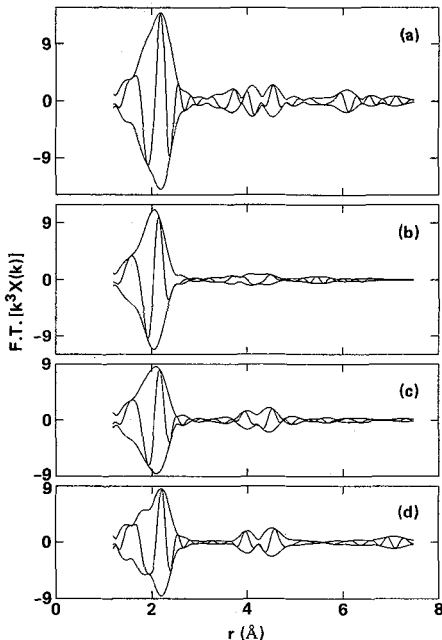


Fig. 1 The Fourier transform of  $k^3 X(k)$  to real space for the EXAFS data on the Mn K-edge at 77K of (a)  $\text{Al}_6\text{Mn}$ , (b)  $a\text{-Al}_{0.85}\text{Mn}_{0.15}$ , (c)  $i\text{-Al}_{0.84}\text{Mn}_{0.16}$  and (d)  $i\text{-Al}_{0.74}\text{Mn}_{0.20}\text{Si}_{0.06}$ . The transform was done using a window from  $k = 2.8$  to  $12.7 \text{ \AA}^{-1}$ , broadened by a Gaussian of width  $0.5 \text{ \AA}^{-1}$ .

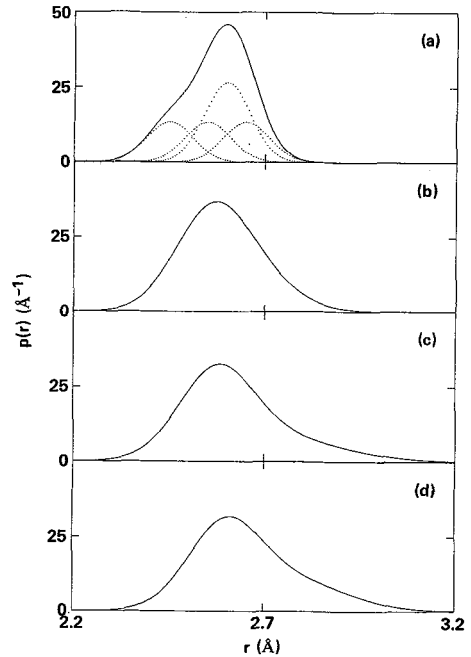


Fig. 2 The near-neighbor pair distribution function for (a) crystalline  $\text{Al}_6\text{Mn}$ , showing the four constituent Gaussian peaks of width  $\sigma = 0.06 \text{ \AA}$ , (b)  $a\text{-Al}_{0.85}\text{Mn}_{0.15}$ , (c)  $i\text{-Al}_{0.84}\text{Mn}_{0.16}$ , and (d)  $i\text{-Al}_{0.74}\text{Mn}_{0.20}\text{Si}_{0.06}$ .

These qualitative comments are borne out by detailed fits to the data. A variety of fits [8] to the data were performed using crystalline  $\text{Al}_6\text{Mn}$  as the structural standard, using a single Mn-Al peak obtained by removing the known asymmetry in the  $p(r)$  of  $\text{Al}_6\text{Mn}$ , and using a single Mn-Al peak derived from theoretical calculations [12]. All three approaches gave consistent results for the first-neighbor Mn-Al pair distribution function,  $p(r)$ . First, a single Mn-Al peak does not fit the i-phase and a-phase data. This indicates that the Mn is not in a single, symmetric site in these materials. Second, a two-peak fit does reproduce the i- and a-phase data. The results, shown in Fig. 2, are a  $p(r)$  that is quite asymmetric for the i-phase and somewhat less so for the a-phase, but both considerably more asymmetric than the known distribution for crystalline  $\text{Al}_6\text{Mn}$  [13]. The total number of Al neighbors is  $10 \pm 1$  in the i-phase and a-phase, 10 in the c-phase. The two peaks that describe the  $p(r)$  of the i- and a-phases could correspond to the following: (1) a single, highly asymmetric near-neighbor distribution for a single Mn site, (2) two inequivalent Mn sites, or (3) several Mn sites with a broad Mn-Al distribution. The second case does not appear likely due to the broad width of the second peak (see Fig. 3). Also, due to small variations we observe in the  $p(r)$  for i- $\text{AlMn}$  of varying Mn content, the third case appears to be the most likely one.

In the two-peak fits to the i-phase data, the first peak is centered at about 2.55 Å, near the mean Mn-Al spacing of 2.57 Å in crystalline  $\text{Al}_6\text{Mn}$ . The position of the second peak varies somewhat depending on the Mn concentration and type of fit but is in the vicinity of 2.72–2.78 Å. These constituent peaks for i- $\text{Al}_{0.84}\text{Mn}_{0.16}$  are shown in Fig. 3. Also shown is the Mn-Al distribution in the dilute alloy, as derived from our EXAFS data. It is centered at 2.79 Å. For display purposes, it is reduced in amplitude by 1/3. Since the second peak in the fit to the i-phase is near that of Mn-Al in dilute  $\text{AlMn}$  alloys and free FCC Al is known to be present in the icosahedral samples, it was necessary to rule out the possibility that this second peak is due to the Al phase. This is readily done on two counts. First, it is too broad by  $\Delta\sigma \approx 0.09$  Å. Second, it is too large in amplitude. It would require about 1/2 of the Mn atoms to be in the dilute alloy phase. This would require the alloy phase to have a 12% Mn content. This is too high since, for the quenching rates used to prepare these samples, only  $\approx 5\%$  can be accommodated in FCC Al before the i-phase forms. So the high- $r$  peak is not due to Mn in FCC Al but rather is part of the  $p(r)$  of the i-phase.

As noted in Fig. 2, the i-phase and a-phase have near-neighbor Mn-Al distributions that are substantially more asymmetric than that of the crystalline phase. To this extent, the i- and a-phases are similar. Also, they both have  $10 \pm 1$  Al neighbors to each Mn. There are some small differences, however, as seen in Fig. 4. The a-phase has a distribution with somewhat less asymmetry. This indicates that the structural units that form the two phases are similar but that the a-phase has fewer Al neighbors at higher distances. This result agrees with the NMR [6] and Mossbauer [5] conclusions that the distribution of electric field gradients at the transition metal site in the a- and i-phases is comparable.

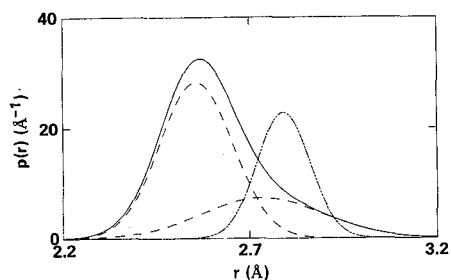


Fig. 3 The individual peaks (dashed line) in the two-peak fit to i- $\text{Al}_{0.84}\text{Mn}_{0.16}$  that make up the total distribution (solid line). The dot-dash curve is the Mn-Al first neighbor  $p(r)$  for dilute Mn in FCC Al, scaled by 1/3.

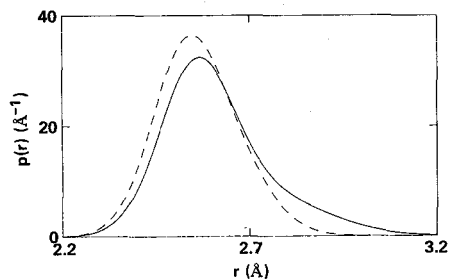


Fig. 4 The first-neighbor pair distribution function for i- $\text{Al}_{0.84}\text{Mn}_{0.16}$  (solid line) and a- $\text{Al}_{0.85}\text{Mn}_{0.15}$  (dashed line).

Acknowledgments: We would like to thank T. Egami, R. Gronsky and J. Mikkelsen, Jr., for providing the Al-Mn quasicrystals and alloys, F. Ponce for the TEM measurements, and the staff at Stanford Synchrotron Radiation Laboratory (SSRL) for their assistance. The experiments were performed at SSRL, Stanford University, which is supported by the U.S. Department of Energy, Office of Basic Sciences, and the National Institute of Health, Biotechnology Resource Division. This research was supported in part by National Science Foundation Grant No. DMR 85-05549.

### References

- [1] SHECHTMAN, D., BLECH, I., GRATIAS, D., CAHN, J. W., *Phys. Rev. Lett.* **53** (1984) 1951.
- [2] POON, S. J., DREHMAN, A. J., LAWLESS, K. R., *Phys. Rev. Lett.* **55** (1985) 2324.
- [3] LEVINE, D., STEINHARDT, P. J., *Phys. Rev. Lett.* **53** (1984) 2477.
- [4] PAULING, L., *Nature* **317** (1985) 512.
- [5] SWARTZENDRUBER, L. J., SHECHTMAN, D., BENDERSKY, L., CAHN, J. W., *Phys. Rev. B* **32** (1985) 1383; EIBSCHUTZ, M., CHEN, H. S., HAUSER, J. J., *Phys. Rev. Lett.* **56** (1986) 169.
- [6] WARREN, W. W., Jr., CHEN, H. S., HAUSER, J. J., *Phys. Rev. B* **32** (1985) 7614; RUBENSTEIN, M., STAUSS, G. H., PHILLIPS, T. E., MOORJANI, K., BENNETT, L. H., *J. Mater. Res.* **1** (1986) 243.
- [7] STERN, E. A., MA, Y., BOULDIN, C. E., *Phys. Rev. Lett.* **55** (1985) 2172.
- [8] BOYCE, J. B., MIKKELSEN, J. C., Jr., BRIDGES, F. G., EGAMI, T., *Phys. Rev. B* **33** (1986) 7314.
- [9] MARCUS, M. A., CHEN, H. S., ESPINOSA, G. P., TSAI, C. L. *Solid State Commun.* **58** (1986) 227.
- [10] SADO, A., FLANK, A. M., LAGARDE, P., SAINFORT, P., BELLISSENT, R., *J. Physique* **47** (1986) 105.
- [11] HAYES, T. M., BOYCE, J. B., in *Solid State Physics*, Vol. 37 (Academic Press, New York, 1982), pp. 173-351.
- [12] TEO, B. K., LEE, P. A., *J. Am. Chem. Soc.* **101** (1979) 2815.
- [13] KONTIO, A., COPPENS, P., *Acta Cryst. B* **37** (1981) 433.